

Generalized concurrence and quantum phase transition in spin-1 Heisenberg model

H Bahmani, G Najarbashi and A Tavana

Department of Physics, University of Mohaghegh Ardabili, Ardabil 179, Iran

E-mail: najarbashi@uma.ac.ir

Received 27 July 2019, revised 5 December 2019

Accepted for publication 10 December 2019

Published 24 February 2020



Abstract

In this paper we investigate the ability of the generalized concurrence as a quantum entanglement measure to describe the quantum and thermal phase transitions in the spin-1 Heisenberg model with bilinear and biquadratic interactions and single-ion anisotropy terms, under a magnetic field. Calculations are performed for two and three spin chains based on the exact diagonalization method. We show that in the near vicinity of the zero temperature, the generalized concurrence changes abruptly from a finite non-zero value to zero by changing the parameters of the model. This is signature of a quantum phase transition that is carefully justified by studying the thermodynamic functions such as magnetization, particle number, particle susceptibility and magnetic susceptibility. The critical points are found and various ordered phases are discussed.

Keywords: concurrence, quantum phase transition, entanglement

(Some figures may appear in colour only in the online journal)

1. Introduction

Quantum phase transition (QPT) is a pure quantum phenomenon that is an abrupt change in the ground state of the system when a non-thermal parameter of the model, e.g. an external field, is continuously changing. QPT is usually associated with non-analyticity in physical properties of systems. This phase change is derived by quantum fluctuations which, in contrast to thermal fluctuations, exist at zero temperature according to the uncertainty principle of Heisenberg [1]. In recent decades, studies on QPTs have grown considerably by the means of ideas and tools of quantum information science [2, 3]. In this context, new concepts based on quantum entanglement or, generally, quantum correlations has been put forward. The claim is that different quantum correlations such as concurrence [3–5], negativity [6], fidelity [7, 8], quantum discord [9–14], etc can describe critical behaviors like scaling, critical points and critical exponents [2, 3, 15–17]. Currently, serious attempts are being devoted to discover entanglements in condensed matter systems which can be utilized in quantum communications and information science. So, it is very intriguing to study entanglements in solid state systems, specially, in spin chains [18–24] which can mimic various physical phenomena

because of their rich entanglement features [25, 26]. Entanglements present at nonzero temperatures are called thermal entanglements, which refer to the entanglements of mixed states of a multi component system in the thermal equilibrium. This concept has been introduced as a resource in quantum information processes since it demonstrates non-local quantum correlations in a thermal system [27].

The concurrence measure, introduced by Hill and Wootters [4], has acquired intense attention because of its ability in characterizing the amount of entanglement in pure and mixed two-qubit states. Concurrence is usually used to study QPTs in various interacting spin-cell [28, 29] or many-body systems [21, 30–32]. In higher dimensions, attempts have been performed to understand or interpret the generalized concurrence [33–39]. For example, Uhlmann generalized Wootters's concurrence to characterize the degree of entanglement in arbitrary Hilbert spaces, as discussed in detail in [33]. For the pure state $|\psi\rangle$, the generalized concurrence on the subspaces H_A and H_B of the total Hilbert space $H = H_A \otimes H_B$ is defined by $C(|\psi\rangle) = \sqrt{2(1 - \text{Tr } \rho_A^2)}$, where ρ_A is the reduced density matrix obtained by tracing over the subspace H_B [34]. The generalized concurrence of the mixed state ρ is defined as a convex roof, $C(\rho) = \min_{\sum_i p_i |\psi_i\rangle} \sum_i p_i C(|\psi_i\rangle)$, where the minimization is

done over all realization $\rho = \sum p_i |\psi_i\rangle \langle \psi_i|$ with $p_i \geq 0$, and $C(|\psi_i\rangle)$ is the concurrence of the pure state $|\psi_i\rangle$. Based on generalized concurrence and using the concept of the graph in mathematics, Akhound *et al* classified the entanglement in graph qubit states. Results showed that the the generalized concurrence is a suitable measure of entanglement for multi-qubit graph states [40]. Chang *et al* found out that the upper bound of the violation of the Bell's inequality for a two-qubit state can be generalized to n-qubit systems. They showed that the upper bound of the violation of the Bell's inequality is given in terms of generalized concurrence provided that there exists a state in terms of two variables [41].

Considering quantum field theory in curved spacetimes, Martín-Martínez *et al* discussed the entanglement occurring in quantum fields. They explored how their results regarding production of entanglement, are affected by the statistics of the field, the type of expansion, and the coupling to spacetime curvature. They used the von Neumann entropy of the reduced state of a bipartite pure state to quantify the entanglement [42, 43]. Also, Martín-Martínez *et al* showed that studying the vacuum entanglement of a scalar field via concurrence and negativity measures, can identify the spacetime topology [44]. Whereas entanglement has been intensively investigated in bipartite quantum states, the situation becomes, increasingly, difficult as we deal with multipartite quantum systems. In the realm of multipartite quantum systems, based on Greenberger–Horne–Zeilinger (GHZ)-like state, Qiang *et al* utilizing genuine multipartite concurrence investigated entanglement properties of Dirac fields in non-inertial frames. They evaluated analytical concurrences for bipartite and tripartite entanglements. Also, they showed that all tripartite systems of Dirac fields in noninertial fields are monogamous [45]. Qiang *et al* applied genuine multipartite concurrence for the investigation of entanglement properties of three Jaynes–Cummings systems initially putting in GHZ-like state. They calculated analytical concurrence expressions for various subsystems including three atom, three-cavity and some atom-cavity mixed systems. Moreover, they investigated the global system and clarified the evolution of its concurrence [46].

Among spin-1/2 chain models, the Heisenberg chain is one of the simplest quantum models which is usually considered as the medium for generating quantum entanglements [2, 3, 47–51]. However, spin-1 systems have, naturally, richer phase diagrams and exhibit more complex phenomena and finding their ground state is rather more complicated. There are many studies on the connection between the quantum entanglement and the QPT in spin-1 chains [52–59]. It is proposed that an energy gap opens in one-dimensional Heisenberg spin-integer chains between the ground state and the first excited state, which is called the Haldane gap [60]. The Blume–Emery–Griffiths (BEG) spin-1 Ising model [61, 62], has played a key role in the theory of tricritical points and various quantum phase transitions. Based on the density matrix renormalization group (DMRG) method, Malvezzi *et al* have studied the quantum and classical correlations in the ground states of spin-1 Heisenberg chains [63]. Wang *et al*, have used the concept of negativity to study

the pairwise entanglement of bilinear and bilinear-biquadratic spin-1 Heisenberg models [64]. Ren *et al* have shown that the QPT from the Haldane spin liquid to Neel spin solid can be properly described by the fidelity susceptibility in an anti-ferromagnetic spin-1 XXZ model [65].

Most of the previous works on the thermal entanglement are restricted to spin-1/2 systems. The purpose of this paper is to employ the generalized concurrence defined by Li *et al* [39] to study the entanglement of the thermal state of a spin-1 Heisenberg model with two and three particles, to find the critical QPT points. We show that long-distance entanglements are embodied in the spin-1 Heisenberg chain and its scaling properties are different from the spin-1/2 chain, due to the presence of the Haldane gap. We should note that, although we deal only with few-particle systems, our results of QPTs are generic to actual critical systems where there exist a large number of particles in system. Indeed, evaluated concurrence for two and three spins might have consequences for large quantum critical systems. For real systems including a large number of particles one has to use approximate methods such as Genetic algorithm [66, 67] and DMRG [68, 69]. Here our results are obtained by diagonalization technique for thermal states which reduce in the limit of $T \rightarrow 0$ to the ground states, while approximate methods are only applied for ground states.

The paper is organized as follows. In section 2, we review the spin-1 Heisenberg model, thermal states and the definition of generalized concurrence vector. In section 3, we investigate the effect of main model parameters, i.e. the crystal field, the biquadratic interaction strength and temperature on the entanglement and response functions for anti-ferromagnetic and ferromagnetic couplings, for two-qutrit case. In section 4, the same procedure is performed for the three-qutrit case. Conclusions and results are summarized in section 5.

2. Model and method

Our intention is to illustrate the connection between the generalized concurrence and QPT through a few examples. To this end, we consider the spin-1 Heisenberg model, with bilinear, biquadratic and single-ion anisotropy terms in the presence of a magnetic field, h ,

$$H = \sum_{i=1}^N [J_i(\mathbf{S}_i \mathbf{S}_{i+1}) + \lambda(\mathbf{S}_i \mathbf{S}_{i+1})^2] + D \sum_{i=1}^N (S_i^z)^2 + h \sum_{i=1}^N S_i^z. \quad (2.1)$$

Here \mathbf{S}_i represents the quantum mechanical spin operator vector at lattice site i , and obeys the $SU(2)$ commutator algebra $[S_m^i, S_n^j] = \delta_{mn} \epsilon^{ijk} S_n^k$, (with $i, j = x, y, z$). We adopt cyclic boundary conditions, i.e. $\mathbf{S}_{N+1} = \mathbf{S}_1$, where N is the number of lattice sites. The first term represents the Heisenberg exchange interaction between spins and the sum is over all nearest neighbor links. For simplicity, we restrict ourselves to the case $J_i = J$ for all $i = 1, \dots, N$. D is the value of the longitudinal crystalline field, which is considered to be oriented along the z -axis and usually plays the role of

chemical potential. We will show that the entanglement depends significantly to this parameter. The term λ is the strength of the biquadratic interaction which is meaningful for spins higher than $\frac{1}{2}$, due to the fact that the anti-commutation relation $\{\mathbf{S}_m^i, \mathbf{S}_n^j\} = \frac{1}{2}\delta_{mn}\delta_{ij}$ holds for spin $\frac{1}{2}$.

In statistical mechanics, a canonical ensemble is an ensemble in which the macrostate of the system is expressed in terms of parameters number of particles N , volume V and temperature T . In this ensemble, the system energy E ranges from zero to infinity. The probability P finding a system in the ensemble characterized by the energy value E_i is proportional to $\exp(-\beta E_i)$ where the proportionality constant becomes $\frac{1}{\sum_i \exp(-\beta E_i)}$. The quantity $\sum_i \exp(-\beta E_i)$ is known as the partition function of system which describes the statistical properties of a system in thermodynamic equilibrium. Therefore, a thermal equilibrium state [31, 70–74] in a canonical ensemble is described by the Gibb's density operator. Therefore, a thermal equilibrium state [31, 70–74] in a canonical ensemble is described by the Gibb's density operator

$$\rho(T) = \frac{e^{-\beta H}}{Z} = \sum_i \frac{e^{-\beta E_i}}{Z} |\psi_i\rangle \langle \psi_i|, \quad (2.2)$$

where E_i s are the energy eigenvalues, H is the system Hamiltonian and $Z = \text{Tr}(e^{-\beta H}) = \sum_i e^{-\beta E_i}$ is the partition function, with $\beta = \frac{1}{k_B T}$. For simplicity we take $k_B = 1$. Because of the temperature dependence of the density matrix, $\rho(T)$, this approach to the entanglement problem is known as the thermal entanglement in literature. In many-body systems, quantum entanglement is a special kind of quantum correlations which can be a witness for classical phase transitions, or even for QPTs at finite but small temperatures [75]. There are various measures that quantify the amount of entanglement in both pure and mixed spin- $\frac{1}{2}$ systems. However, because of the lack of an entanglement measure for higher dimensional systems, the entanglement of spin-1 systems have been less investigated [64]. Since the generalized concurrence, introduced previously in [39] and [76], is an important measure of entanglement for qudits, it seems appealing to use it as a witness to detect the entanglement of a mixed density matrix (2.2). The generalized definition of the concurrence measure introduced in [39] is

$$|\mathbf{C}|^2 = \sum_{\alpha\beta} C_{\alpha\beta}^2, \quad (2.3)$$

where $C_{\alpha\beta}$ are the components of the concurrence vector \mathbf{C} defined as :

$$C_{\alpha\beta}(\rho) = \max\{0, 2 \max(\lambda_i^{\alpha\beta}) - \sum_i \lambda_i^{\alpha\beta}\}, \quad (2.4)$$

where $\lambda_i^{\alpha\beta}$ with $i = 1, \dots, 4$ are square roots of the eigenvalues of the matrix $\rho(L_\alpha \otimes L_\beta) \rho^*(L_\alpha \otimes L_\beta)$ where L_α , ($\alpha = 1, \dots, \frac{d_1(d_1-1)}{2}$) and L_β , ($\beta = 1, \dots, \frac{d_2(d_2-1)}{2}$) are generators of $SO(d_1)$ and $SO(d_2)$, respectively. Here ρ^* denotes the complex conjugate of density matrix ρ . If concurrence is equal to zero, the state is unentangled, otherwise it

is entangled. For to the particular spin-1 problem at hand, the explicit form of the generators are

$$L_1 = \begin{pmatrix} 0 & 1 & 0 \\ -1 & 0 & 0 \\ 0 & 0 & 0 \end{pmatrix}, L_2 = \begin{pmatrix} 0 & 0 & -1 \\ 0 & 0 & 0 \\ 1 & 0 & 0 \end{pmatrix}, \\ L_3 = \begin{pmatrix} 0 & 0 & 0 \\ 0 & 0 & 1 \\ 0 & -1 & 0 \end{pmatrix}. \quad (2.5)$$

We discuss two cases with $N = 2$ and $N = 3$, separately.

3. Two qutrit system

In this section, we consider the two-qutrit chain with $N = 2$. By diagonalization of the Hamiltonian matrix, we obtain the eigenvalues and the corresponding eigenvectors as follows

$$E_1 = -2(h - J - \lambda - D), \quad E_2 = -2(J - \lambda - D), \\ E_3 = 2(h + J + \lambda + D), \quad E_4 = -h - 2J + 2\lambda + D, \\ E_5 = h - 2J + 2\lambda + D, \quad E_6 = -h + 2J + 2\lambda + D, \\ E_7 = h + 2J + 2\lambda + D, \quad E_8 = -J + 5\lambda + D - \alpha_0, \\ E_9 = -J + 5\lambda + D + \alpha_0, \quad (3.6)$$

$$|\psi_1\rangle = |22\rangle, \quad |\psi_2\rangle = \frac{1}{\sqrt{2}}(|20\rangle - |02\rangle), \\ |\psi_3\rangle = |00\rangle, \quad |\psi_4\rangle = \frac{1}{\sqrt{2}}(|21\rangle - |12\rangle), \\ |\psi_5\rangle = \frac{1}{\sqrt{2}}(|10\rangle - |01\rangle), \quad |\psi_6\rangle = \frac{1}{\sqrt{2}}(|21\rangle + |12\rangle), \\ |\psi_7\rangle = \frac{1}{\sqrt{2}}(|10\rangle + |01\rangle), \\ |\psi_8\rangle = \frac{1}{\sqrt{2 + \alpha_1^2}}(|02\rangle + \alpha_1|11\rangle + |20\rangle), \\ |\psi_9\rangle = \frac{1}{\sqrt{2 + \alpha_2^2}}(|02\rangle + \alpha_2|11\rangle + |20\rangle), \quad (3.7)$$

where

$$\alpha_0 = \sqrt{9(J - \lambda)^2 - 2(J - \lambda)D + D^2}, \\ \alpha_1 = \frac{J - \lambda - D - \alpha_0}{2(J - \lambda)}, \quad \alpha_2 = \frac{J - \lambda - D + \alpha_0}{2(J - \lambda)}, \quad (3.8)$$

and $|0\rangle$, $|1\rangle$ and $|2\rangle$ are the standard unit vectors in three dimensional Hilbert space, i.e.

$$|0\rangle = \begin{pmatrix} 1 \\ 0 \\ 0 \end{pmatrix}, \quad |1\rangle = \begin{pmatrix} 0 \\ 1 \\ 0 \end{pmatrix}, \quad |2\rangle = \begin{pmatrix} 0 \\ 0 \\ 1 \end{pmatrix}. \quad (3.9)$$

Two eigenvectors $|\psi_1\rangle$ and $|\psi_3\rangle$ are separable pure states while the other eigenvectors are entangled. A straightforward application of Schmidt theorem shows that the maximum entangled state can only be achieved by two $|\psi_8\rangle$ and $|\psi_9\rangle$ states.

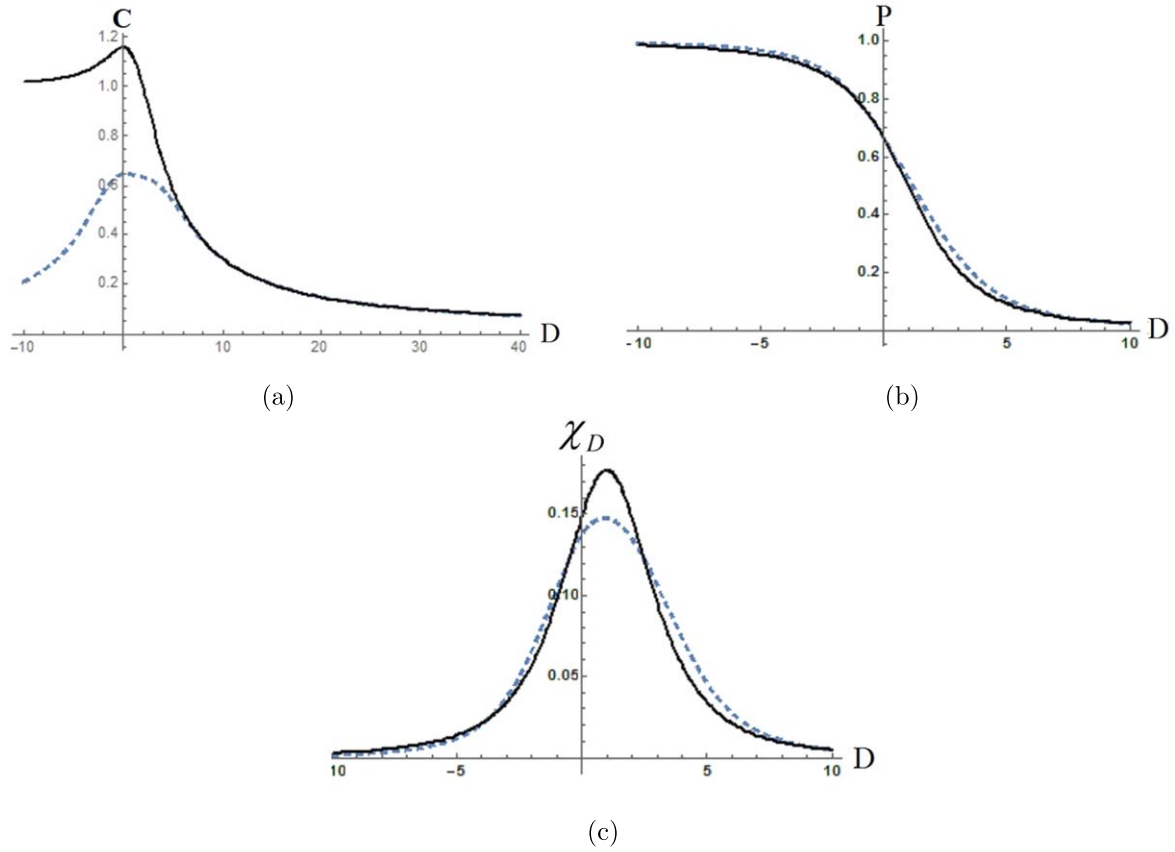


Figure 1. Variations of concurrence (a), particle number (b) and particle susceptibility (c) versus D for $J = 1$, $\lambda = h = 0$ and $N = 2$ with $T = 1$ (dashed) and $T = 0.1$ (solid).

In order to find the quantum critical point in this system, it suffices to investigate particle number, i.e. P , and magnetization, i.e. M , the responses of the thermodynamical potential with respect to D and h , which are defined as

$$P = \langle (S^z)^2 \rangle = -\frac{\partial F}{\partial D}, \quad M = \langle S^z \rangle = -\frac{\partial F}{\partial h}, \quad (3.10)$$

where the expectation values are taken with respect to the thermal density matrix and $F = -T \ln Z$ is the free energy. We also define the particle and the magnetic susceptibilities, respectively as

$$\chi_D = \frac{\partial P}{\partial D}, \quad \chi_h = \frac{\partial M}{\partial h}, \quad (3.11)$$

where χ_D and χ_h are functions that measure the tendency of the medium to respond to the longitudinal crystal field and align with the external magnetic field, respectively.

With this background, let us now discuss in more detail the behavior of the concurrence, particle number, particle susceptibility and magnetic susceptibility at low and high temperatures for two ferromagnetic and anti-ferromagnetic cases. Figure 1 shows the concurrence, the particle number and the particle susceptibility versus D at zero field for anti-ferromagnetic case, i.e. $J = 1$. While the particle number is a monotonic function of D , the concurrence and the particle susceptibility reach to their

maximum values at $D = 0$ and $D > 0$, respectively. Unlike the concurrence and the particle susceptibility, the particle number remains robust with respect to the variations in temperature. Also it is notable that the maximum of the concurrence is larger than one at $D = 0$ for small temperatures, which is an exclusive property of spin-1 systems. In general, C takes its maximum value, $\sqrt{2(d-1)/d}$ when $|\psi\rangle$ is a maximally entangled state in $\mathbb{C}^d \otimes \mathbb{C}^d$ dimensional Hilbert space [76]. In the present case, the non-degenerated maximal entangled state reduces to $|\psi\rangle = \frac{1}{\sqrt{3}}(|02\rangle + |11\rangle + |20\rangle)$ with the maximal concurrence $\sqrt{4/3}$. On the other hand, the concurrence decreases with increasing temperature which means that quantum correlations in the sense of entanglement decreases. This result coincides with the observation for the negativity measure [74].

Let us now analyze the effect of the longitudinal crystalline field D when $J = \lambda = 1$ at zero magnetic field, $h = 0$. As depicted in figure 2, the concurrence and all other response functions yield common critical points at $D \simeq 0$ and $D \simeq 4$. In the limit of large positive D , all functions tend to zero. When $D \rightarrow -\infty$, the concurrence and the particle number take a nonzero fixed value, but the magnetic and the particle susceptibilities vanish.

Figure 3(a) shows a Neel state-like behavior of the magnetic susceptibility in a broad range of D values, where the nearest neighbor spins freeze up anti-parallel to each

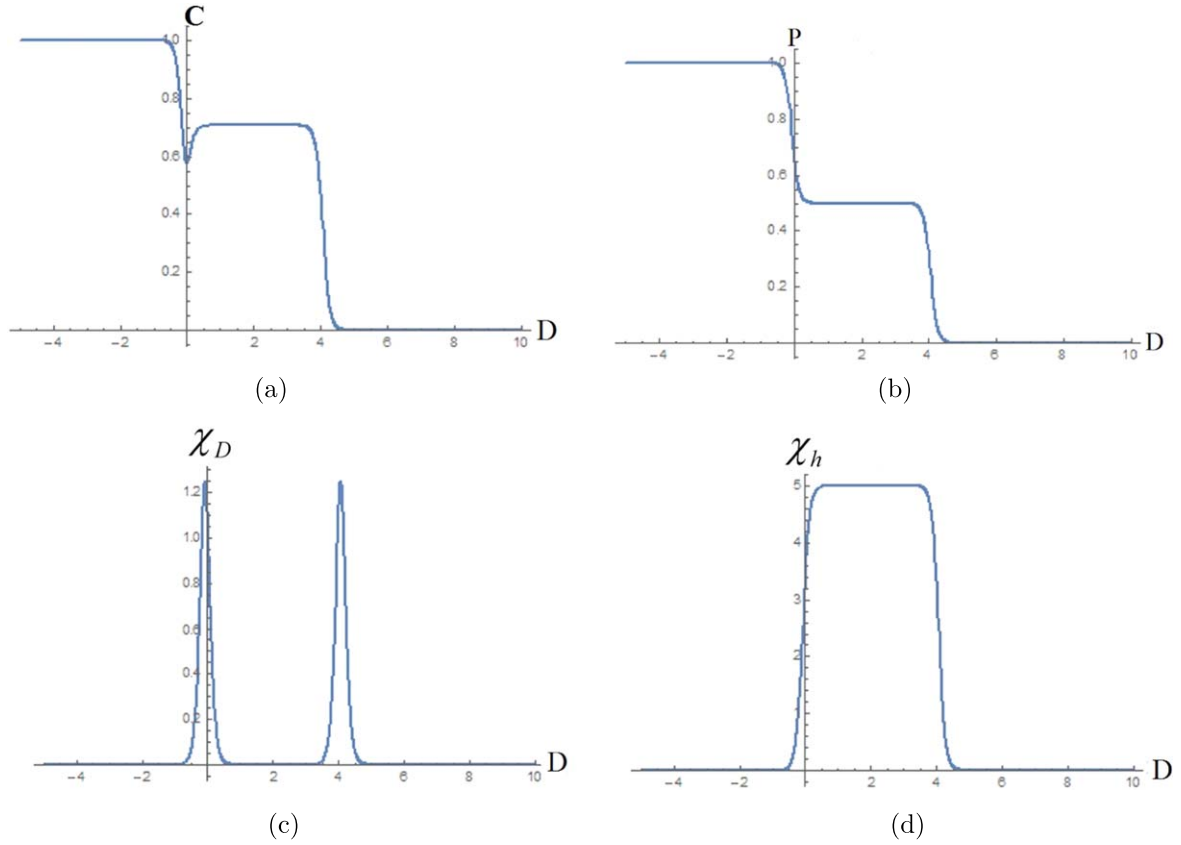


Figure 2. Variation of generalized concurrence (a), particle number (b), particle susceptibility (c) and magnetic susceptibility (d) versus D for $J = 1$, $\lambda = 1$ and $h = 0$ with $N = 2$ at $T = 0.1$.

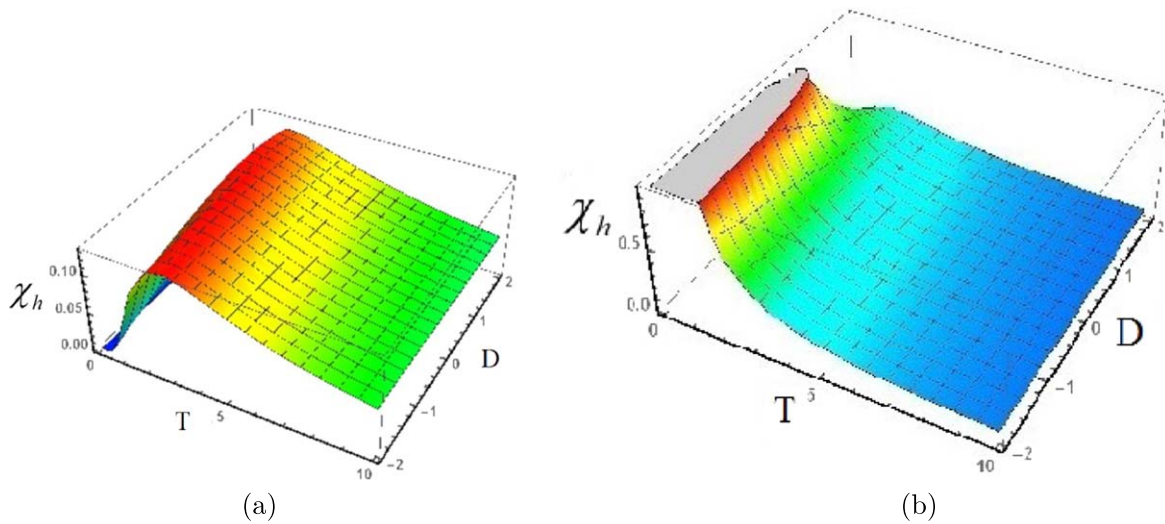


Figure 3. Magnetic susceptibility versus T and D for $J = 1$ (a) and $J = -1$ (b) with $\lambda = 0$, $h = 0$ and $N = 2$.

other. While, in the case of $J = -1$ the Neel state-like behavior will not appear for the whole range of the D values. In other words, the magnetic susceptibility diverges for infinitesimally small temperatures in the ferromagnetic case, as shown in figure 3(b). In order to clarify this behavior, we need to examine other functions in the vicinity of the zero temperature for $J = -1$.

In the ferromagnetic case, i.e. $J = -1$, the Hamiltonian supports configurations that spins at neighboring sites are aligned parallel to each other. It is noticeable that near the vicinity of the zero temperature, the concurrence measure, the particle number, the particle susceptibility and the magnetic susceptibility change abruptly at $D = 0$ that can be a signature of a finite temperature QPT (see figure 4). It is natural

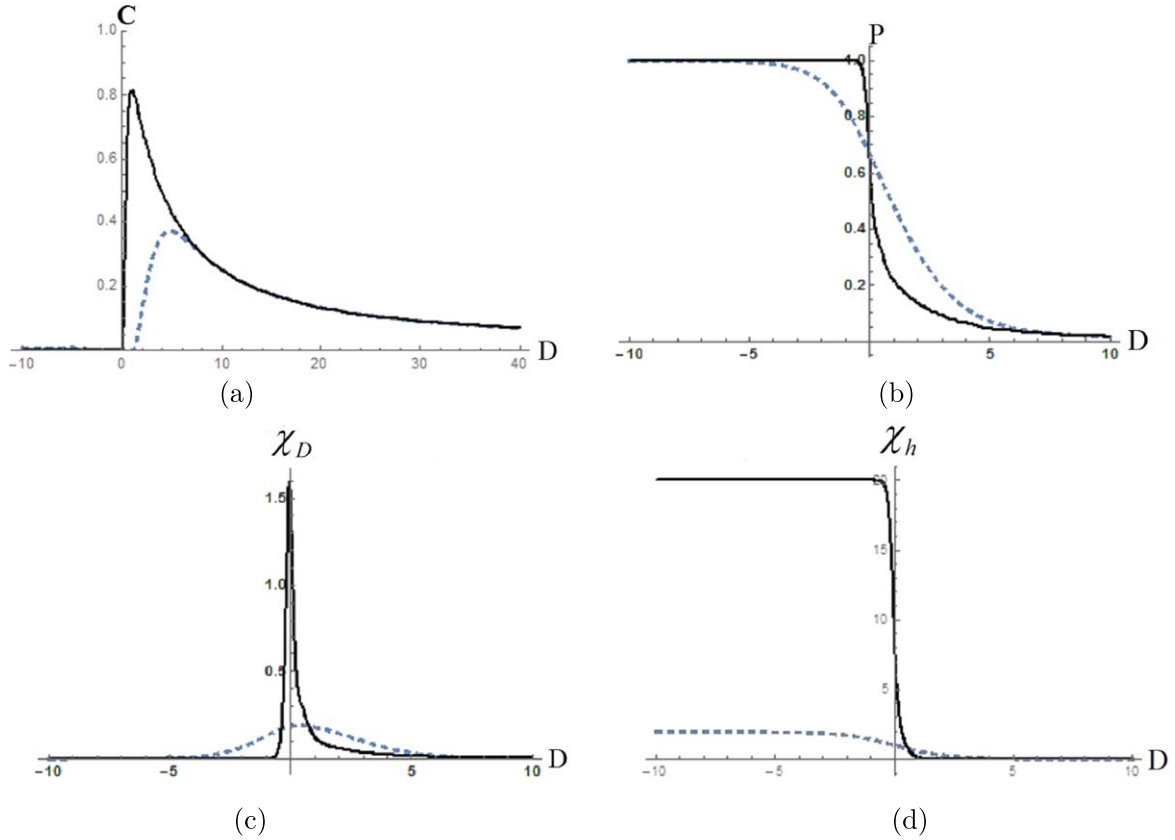


Figure 4. Variations of concurrence (a), particle number (b), particle susceptibility (c) and magnetic susceptibility (d) versus D for $J = -1$, $\lambda = h = 0$ and $N = 2$ with $T = 1$ (dashed) and $T = 0.1$ (solid).

to describe the ordered phase in terms of the concurrence which indicates two distinct separable and entangled phases. At infinitesimal T both the concurrence and the particle susceptibility vanish for $D < 0$, while the particle number and the magnetic susceptibility saturate at their maximum value. For small positive D , all of the studied functions tend to zero for the whole temperature range. For $D = 0$, the ground state is fivefold degenerated including $|\psi_1\rangle$, $|\psi_3\rangle$, $|\psi_6\rangle$, $|\psi_7\rangle$ and $|\psi_8\rangle$ states with the zero concurrence.

Let us now consider the effects of biquadratic interaction term on the thermodynamic functions and on the concurrence at low and high temperatures. Figure 5 shows that all of the intended functions display a critical point at $\lambda \simeq 0.3$ which in turn implies that the system undergoes a first order phase transition at low temperatures. We note that the average energy vanishes at $\lambda \simeq 0.3$ and its derivative is discontinuous at this point. Once again, concurrence decreases by increasing the temperature. In contrast, as the temperature is lowered, the particle number, P , becomes small, as shown in figure 5(b). For $\lambda \rightarrow -\infty$, each of the studied functions converge to a common value, independent of the temperature, while for $\lambda \rightarrow +\infty$ they get fixed but different values at different temperatures. Similar results hold for $J = -1$ except for that all functions show the critical point at $\lambda = -1$ as depicted in figure 6.

In figure 7 the variation of the concurrence, the magnetization and the particle susceptibility is depicted for different

values of T as a function of h for the anti-ferromagnetic case. The appearance of the critical point at $h_c \simeq \pm 1.83$ shows a QPT at low temperatures. Both the concurrence and the particle susceptibilities achieve their maximum values in the region $h \in [-1.83, 1.83]$ and decrease by increasing the temperature. The absolute value of the magnetization behaves in opposite. For most of the situations, at small magnetic fields magnetization is proportional to the applied magnetic field, i.e. $M \propto h$. For $h \rightarrow \pm\infty$ all functions tend to a constant value, independent of the temperature. For the ferromagnetic case we have four critical points at $h_c^1 \simeq \pm 1$ and $h_c^2 \simeq \pm 0.45$ as depicted in figure 8. Unlike the anti-ferromagnetic case, here the particle susceptibility diverges in the near vicinity of the critical points. At low temperatures the maximum of the concurrence occurs in the intervals $h \in [-1, -0.45]$ and $h \in [0.45, 1]$, and for higher temperature, i.e. $T = 0.1$, the maximum lies in the interval $h \in [-0.45, 0.45]$. The linearity of the magnetization at low magnetic fields is preserved in this case. If we compare the behavior of the concurrence with respect to temperature for two cases $J = \pm 1$, we see two differences; First, the concurrence of the ground state $|\psi_8\rangle$, with $C = \frac{\sqrt{5}}{2}$, $E_8 = -\sqrt{8}$ and $\alpha_1 = -\sqrt{2}$ for $J = 1$ is larger than the concurrence of the state $|\psi_8\rangle$ with $C = \sqrt{1 - \frac{1}{2\sqrt{3}}}$, $E_8 = 2 - \sqrt{12}$ and $\alpha_1 = 1 + \sqrt{3}$, for $J = -1$ at low temperatures. Second, the threshold temperature for $J = -1$, where the concurrence

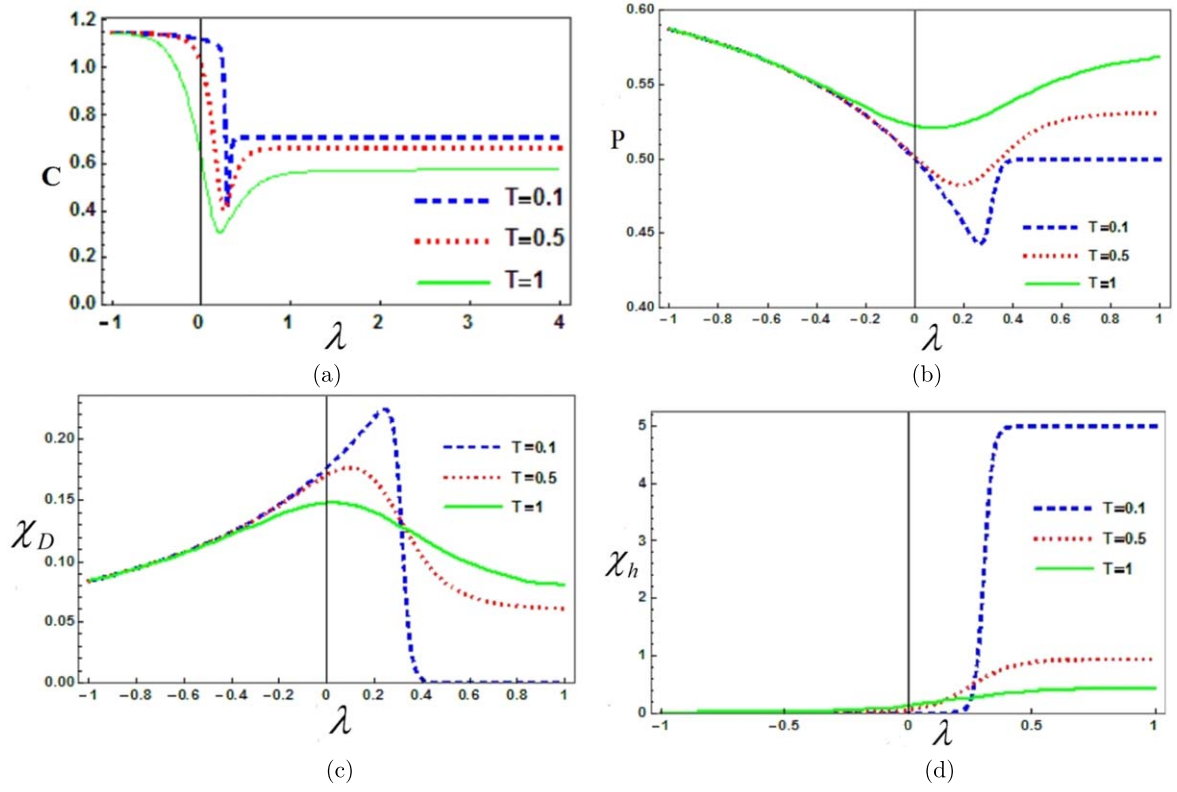


Figure 5. Variation of concurrence (a), particle number (b), particle susceptibility (c) and magnetic susceptibility (d) versus λ for $N = 2$ with $J = D = 1$ and $h = 0$.

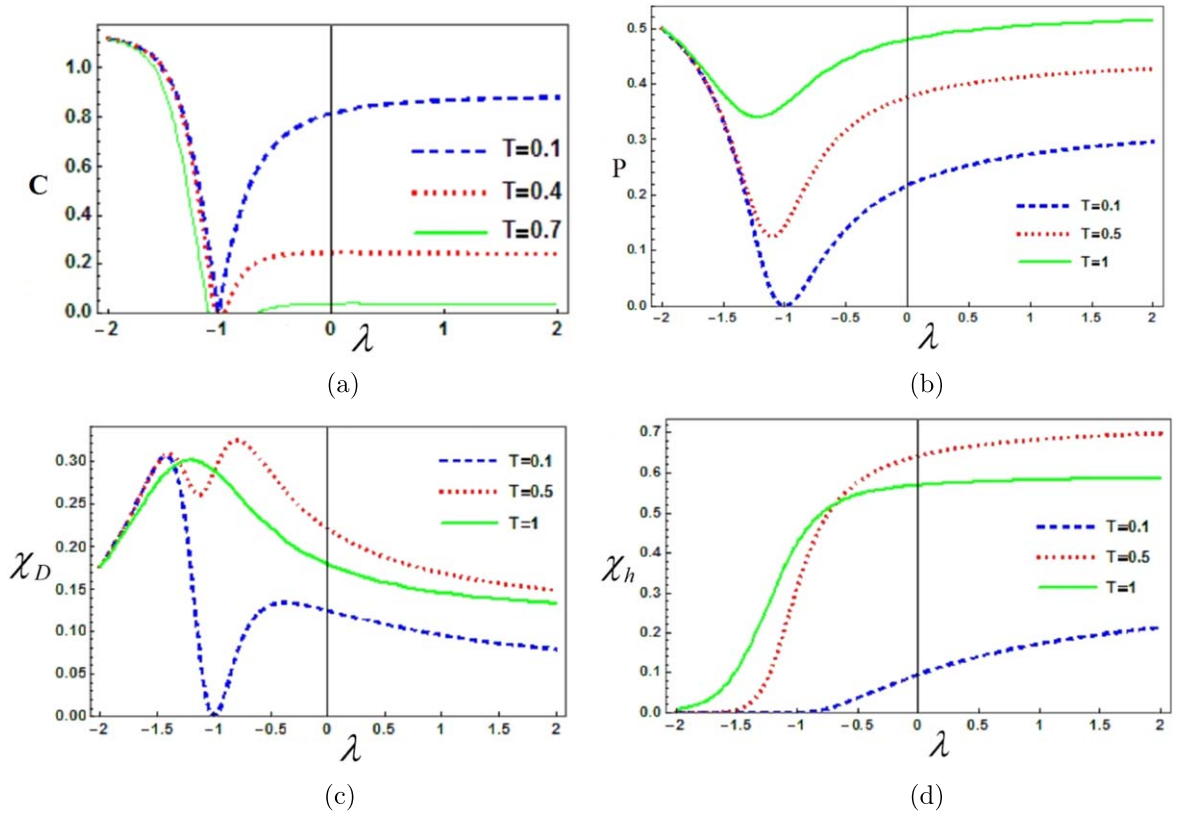


Figure 6. Variation of concurrence (a), particle number (b), particle susceptibility (c) and magnetic susceptibility (d) versus λ for $N = 2$ with $J = -1$, $D = 1$ and $h = 0$.

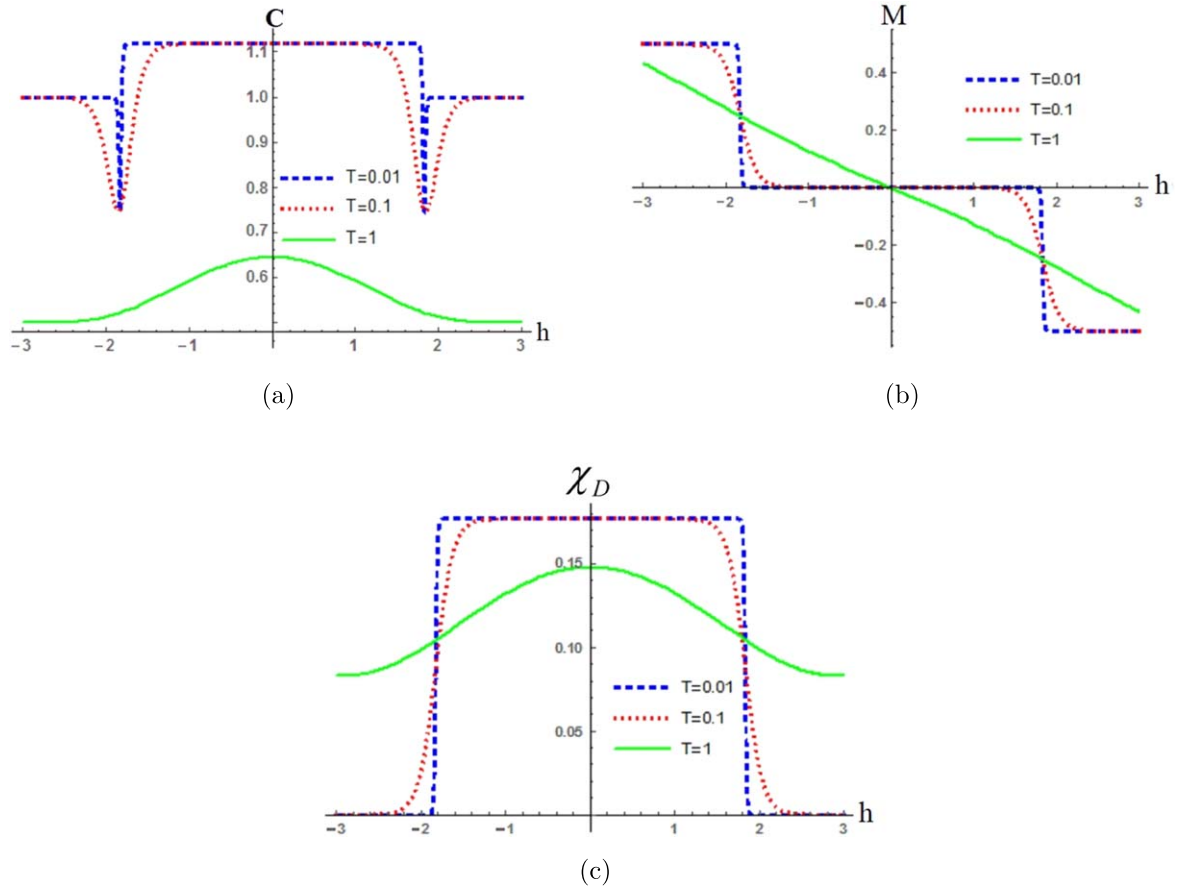


Figure 7. Variation of concurrence (a), magnetization (b) and particle susceptibility (c) versus h for $N = 2$ with $J = D = 1$ and $\lambda = 0$.

vanishes, is smaller than that for $J = 1$ case. In other words, $C(J = 1)$ shows more robustness in comparison with C ($J = -1$) respect to temperature, as shown in figure 9(a). The particle number for $J = 1$ is larger than that for $J = -1$, and they converge to a common value at high temperatures, as shown in figure 9(b). The response functions behave oppositely, i.e. for a broad range of temperatures the particle and the magnetic susceptibilities in the $J = -1$ case are larger than in the $J = 1$ case, except for the particle susceptibility at low temperatures, as depicted in figures 9(c) and (d).

In figure 10, the general behavior of concurrence and response functions are depicted for very low temperature, i.e. $T = 0.01$, in the absence of the biquadratic and the magnetic terms, i.e. $\lambda = h = 0$. For $J < 0$ and $D < 0$, both the concurrence and the particle susceptibility vanish and for $D > 0$ they increase, rapidly. The behavior of the particle number and the magnetic susceptibility is opposite, in the sense that both reach to their maximum value and then rapidly decrease for $D > 0$.

4. Three qutrit system

To keep our discussion simple and generic in scope, we focus on a three-spin-1 chain ($N = 3$) and explore the physical

properties of the system described by the thermal density matrix (2.2). By restricting our investigations to the low temperatures limit, we compare the critical points of the response functions for $N = 3$ case with $N = 2$. The eigenvalues for $N = 3$ are:

$$\begin{aligned}
 E_1 &= 3(h + D + J + \lambda), \\
 E_2 &= -3h + 3D + 3J + 3\lambda, \\
 E_3 &= E_4 = 2D + 3\lambda, \\
 E_5 &= E_6 = -2h + 2D + 3\lambda, \\
 E_7 &= E_8 = 2h + 2D + 3\lambda, \\
 E_9 &= -3J + 2D + 3\lambda, \\
 E_{10} &= -2h + 2D + 3J + 3\lambda, \\
 E_{11} &= 2h + 2D + 3J + 3\lambda, \\
 E_{12} &= E_{13} = -2J + 2D + 5\lambda, \\
 E_{14} &= E_{15} = -h + 2D - J + 4\lambda \\
 &\quad - \sqrt{D^2 + J^2 - 2J\lambda + \lambda^2}, \\
 E_{16} &= E_{17} = h + 2D - J + 4\lambda \\
 &\quad - \sqrt{D^2 + J^2 - 2J\lambda + \lambda^2}, \\
 E_{18} &= E_{19} = -h + 2D - J + 4\lambda \\
 &\quad + \sqrt{D^2 + J^2 - 2J\lambda + \lambda^2}, \\
 E_{20} &= E_{21} = h + 2D - J + 4\lambda \\
 &\quad + \sqrt{D^2 + J^2 - 2J\lambda + \lambda^2},
 \end{aligned}$$

$$\begin{aligned}
E_{22} &= \frac{1}{2}(2D + J + 11\lambda \\
&\quad - \sqrt{4D^2 + 4DJ + 25J^2 - 4D\lambda - 50J\lambda + 25\lambda^2}), \\
E_{23} &= \frac{1}{2}(2D + J + 11\lambda \\
&\quad + \sqrt{4D^2 + 4DJ + 25J^2 - 4D\lambda - 50J\lambda + 25\lambda^2}), \\
E_{24} &= \frac{1}{2}(-2h + 4D + J + 11\lambda \\
&\quad - \sqrt{4D^2 - 12DJ + 25J^2 + 12D\lambda - 50J\lambda + 25\lambda^2}), \\
E_{25} &= \frac{1}{2}(2h + 4D + J + 11\lambda \\
&\quad - \sqrt{4D^2 - 12DJ + 25J^2 + 12D\lambda - 50J\lambda + 25\lambda^2}), \\
E_{26} &= \frac{1}{2}(-2h + 4D + J + 11\lambda \\
&\quad + \sqrt{4D^2 - 12DJ + 25J^2 + 12D\lambda - 50J\lambda + 25\lambda^2}), \\
E_{27} &= \frac{1}{2}(2h + 4D + J + 11\lambda \\
&\quad + \sqrt{4D^2 - 12DJ + 25J^2 + 12D\lambda - 50J\lambda + 25\lambda^2}),
\end{aligned} \tag{4.12}$$

and the corresponding eigenvectors are:

$$\begin{aligned}
|\psi_1\rangle &= |000\rangle, \quad |\psi_2\rangle = |222\rangle, \\
|\psi_3\rangle &= \frac{1}{2}(-|012\rangle - |102\rangle + |120\rangle + |210\rangle), \\
|\psi_4\rangle &= \frac{1}{2}(-|021\rangle + |102\rangle + |120\rangle + |201\rangle), \\
|\psi_5\rangle &= \frac{1}{\sqrt{2}}(-|122\rangle + |221\rangle), \\
|\psi_6\rangle &= \frac{1}{\sqrt{2}}(-|122\rangle + |212\rangle), \\
|\psi_7\rangle &= \frac{1}{\sqrt{2}}(-|001\rangle + |100\rangle), \\
|\psi_8\rangle &= \frac{1}{\sqrt{2}}(-|001\rangle + |010\rangle), \\
|\psi_9\rangle &= \frac{1}{\sqrt{6}}(-|012\rangle + |021\rangle + |102\rangle - |120\rangle - |201\rangle + |210\rangle), \\
|\psi_{10}\rangle &= \frac{1}{\sqrt{3}}(|122\rangle + |212\rangle + |221\rangle), \\
|\psi_{11}\rangle &= \frac{1}{\sqrt{3}}(|001\rangle + |010\rangle + |100\rangle), \\
|\psi_{12}\rangle &= \frac{1}{2}(|012\rangle - |102\rangle - |120\rangle + |210\rangle), \\
|\psi_{13}\rangle &= \frac{1}{2}(|021\rangle - |102\rangle - |120\rangle + |201\rangle), \\
|\psi_{14}\rangle &= \frac{1}{\sqrt{\eta_1^2 + \eta_2^2 + \eta_3^2 + 1}}(\eta_1|112\rangle + \eta_2|121\rangle \\
&\quad + \eta_3|202\rangle + |220\rangle), \\
|\psi_{15}\rangle &= \frac{1}{\sqrt{\eta_4^2 + \eta_5^2 + 2}}(\eta_4|022\rangle - |121\rangle + \eta_5|202\rangle + |211\rangle),
\end{aligned}$$

$$\begin{aligned}
|\psi_{16}\rangle &= \frac{1}{\sqrt{\eta_6^2 + \eta_7^2 + 2}}(\eta_6|011\rangle - |020\rangle + \eta_7|101\rangle + |200\rangle), \\
|\psi_{17}\rangle &= \frac{1}{\sqrt{\eta_8^2 + \eta_9^2 + \eta_{10}^2 + 1}}(\eta_8|002\rangle + \eta_9|020\rangle \\
&\quad + \eta_{10}|101\rangle + |110\rangle), \\
|\psi_{18}\rangle &= \frac{1}{\sqrt{\eta_{11}^2 + \eta_{12}^2 + \eta_{13}^2 + 1}}(\eta_{11}|112\rangle + \eta_{12}|121\rangle \\
&\quad + \eta_{13}|202\rangle + |220\rangle), \\
|\psi_{19}\rangle &= \frac{1}{\sqrt{\eta_{14}^2 + \eta_{15}^2 + 2}}(\eta_{14}|022\rangle - |121\rangle + \eta_{15}|202\rangle + |211\rangle), \\
|\psi_{20}\rangle &= \frac{1}{\sqrt{\eta_{16}^2 + \eta_{17}^2 + 2}}(\eta_{16}|011\rangle - |020\rangle + \eta_{17}|101\rangle + |200\rangle), \\
|\psi_{21}\rangle &= \frac{1}{\sqrt{\eta_{18}^2 + \eta_{19}^2 + \eta_{20}^2 + 1}}(\eta_{18}|002\rangle + \eta_{19}|020\rangle \\
&\quad + \eta_{20}|101\rangle + |110\rangle), \\
|\psi_{22}\rangle &= \frac{1}{\sqrt{\eta_{21}^2 + \eta_{22}^2 + \eta_{23}^2 + \eta_{24}^2 + \eta_{25}^2 + \eta_{26}^2 + 1}} \\
&\quad \times \left(\eta_{21}|012\rangle + \eta_{22}|021\rangle + \eta_{23}|102\rangle + \eta_{24}|111\rangle + \right. \\
&\quad \left. + \eta_{25}|120\rangle + \eta_{26}|201\rangle + |210\rangle \right), \\
|\psi_{23}\rangle &= \frac{1}{\sqrt{\eta_{27}^2 + \eta_{28}^2 + \eta_{29}^2 + \eta_{30}^2 + \eta_{31}^2 + \eta_{32}^2 + 1}} \\
&\quad \times \left(\eta_{27}|012\rangle + \eta_{28}|021\rangle + \eta_{29}|102\rangle + \eta_{30}|111\rangle + \right. \\
&\quad \left. + \eta_{31}|120\rangle + \eta_{32}|201\rangle + |210\rangle \right), \\
|\psi_{24}\rangle &= \frac{1}{\sqrt{\eta_{33}^2 + \eta_{34}^2 + \eta_{35}^2 + \eta_{36}^2 + \eta_{37}^2 + 1}} \\
&\quad \times \left(\eta_{33}|022\rangle + \eta_{34}|112\rangle + \eta_{35}|121\rangle + \right. \\
&\quad \left. + \eta_{36}|202\rangle + \eta_{37}|211\rangle + |220\rangle \right), \\
|\psi_{25}\rangle &= \frac{1}{\sqrt{\eta_{38}^2 + \eta_{39}^2 + \eta_{40}^2 + \eta_{41}^2 + 2}} \\
&\quad \times \left(|002\rangle + \eta_{38}|011\rangle + \eta_{39}|020\rangle + \right. \\
&\quad \left. + \eta_{40}|101\rangle + \eta_{41}|110\rangle + |200\rangle \right), \\
|\psi_{26}\rangle &= \frac{1}{\sqrt{\eta_{42}^2 + \eta_{43}^2 + \eta_{44}^2 + \eta_{45}^2 + \eta_{46}^2 + 1}} \\
&\quad \times \left(\eta_{42}|022\rangle + \eta_{43}|112\rangle + \eta_{44}|121\rangle + \right. \\
&\quad \left. + \eta_{45}|202\rangle + \eta_{46}|211\rangle + |220\rangle \right), \\
|\psi_{27}\rangle &= \frac{1}{\sqrt{\eta_{47}^2 + \eta_{48}^2 + \eta_{49}^2 + \eta_{50}^2 + 2}} \\
&\quad \times \left(|002\rangle + \eta_{47}|011\rangle + \eta_{48}|020\rangle + \right. \\
&\quad \left. + \eta_{49}|101\rangle + \eta_{50}|110\rangle + |200\rangle \right),
\end{aligned}$$

where η_i 's are functions of the intrinsic parameters of the Hamiltonian, i.e. J , λ , h and D . Note that $|\psi_1\rangle$ and $|\psi_2\rangle$ are three-partite separable while the states like $|\psi_5\rangle$ and $|\psi_6\rangle$ are biseparable. With biseparability we mean that the three-partite

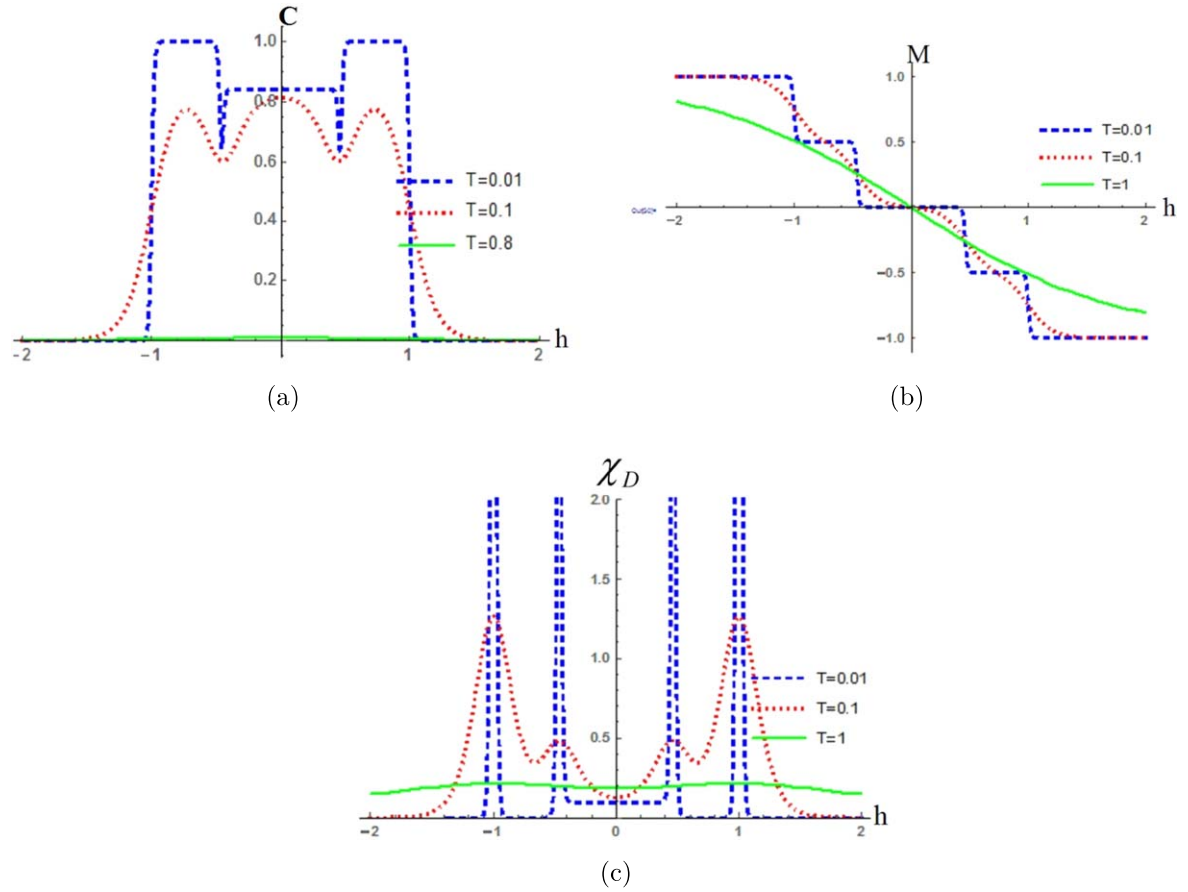


Figure 8. Variation of concurrence (a), magnetization (b) and particle susceptibility (c) versus h for $N = 2$ with $J = -1$, $D = 1$ and $\lambda = 0$.

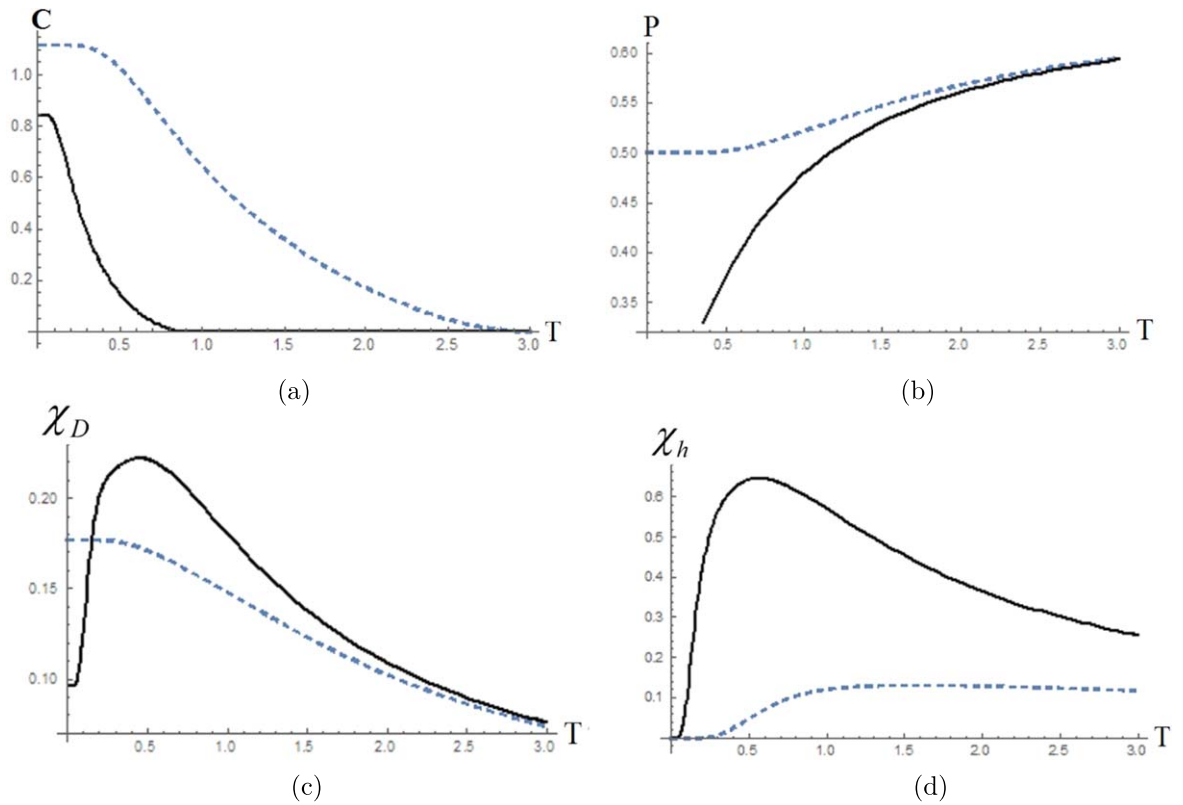


Figure 9. Variation of concurrence (a), particle number (b), particle susceptibility (c) and magnetic susceptibility (d) versus T for $D = 1$, $\lambda = h = 0$ and $N = 2$ with $J = 1$ (dashed) and $J = -1$ (solid).

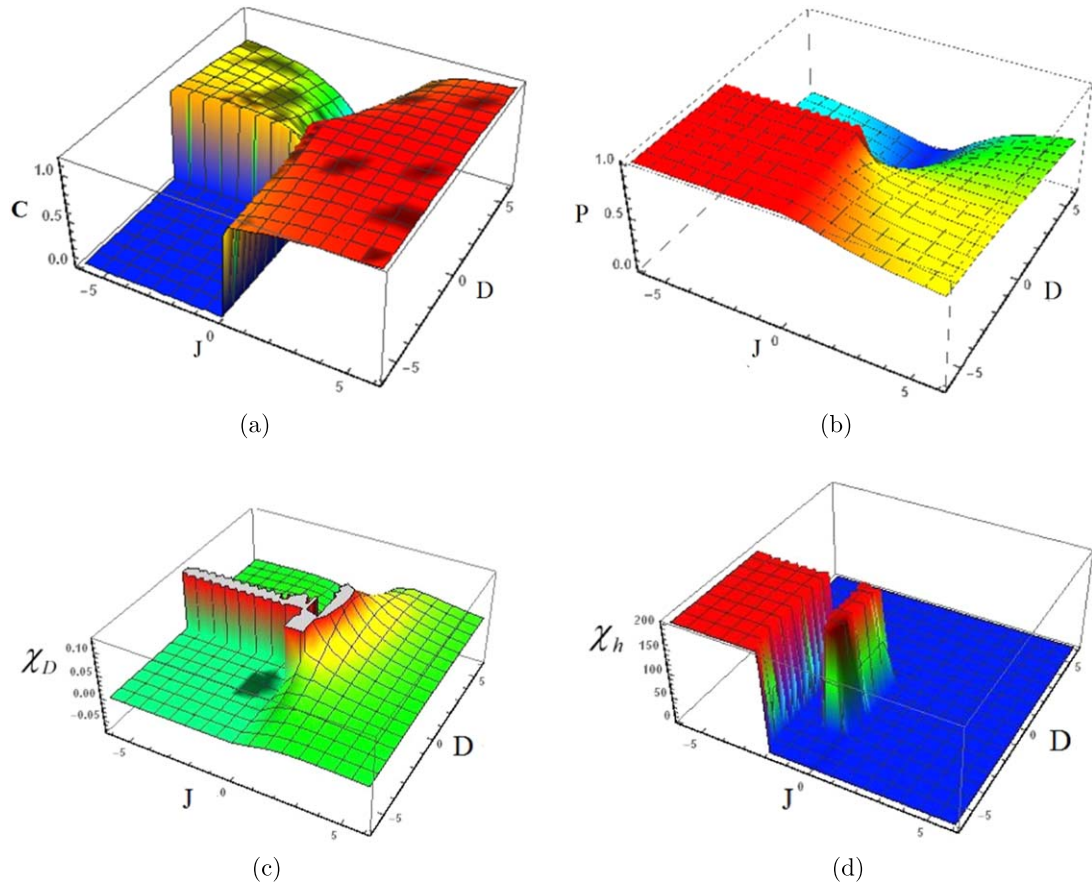


Figure 10. 3-dimensional plot of concurrence (a), particle number (b), particle susceptibility (c) and magnetic susceptibility (d) versus J and D for $N = 2$ with $\lambda = h = 0$ at $T = 0.01$.

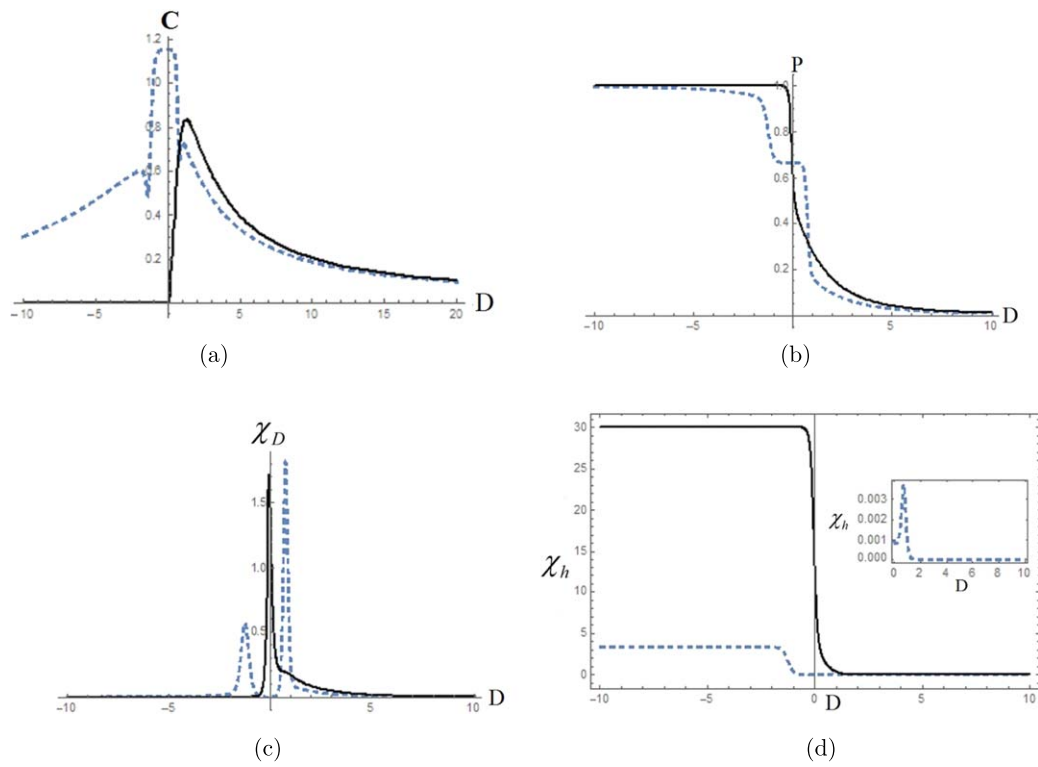


Figure 11. Variations of concurrence (a), particle number (b), particle susceptibility (c) and magnetic susceptibility (d) versus D for $\lambda = h = 0$ and $N = 3$ with $J = 1$ (dashed) and $J = -1$ (solid) at $T = 0.1$.

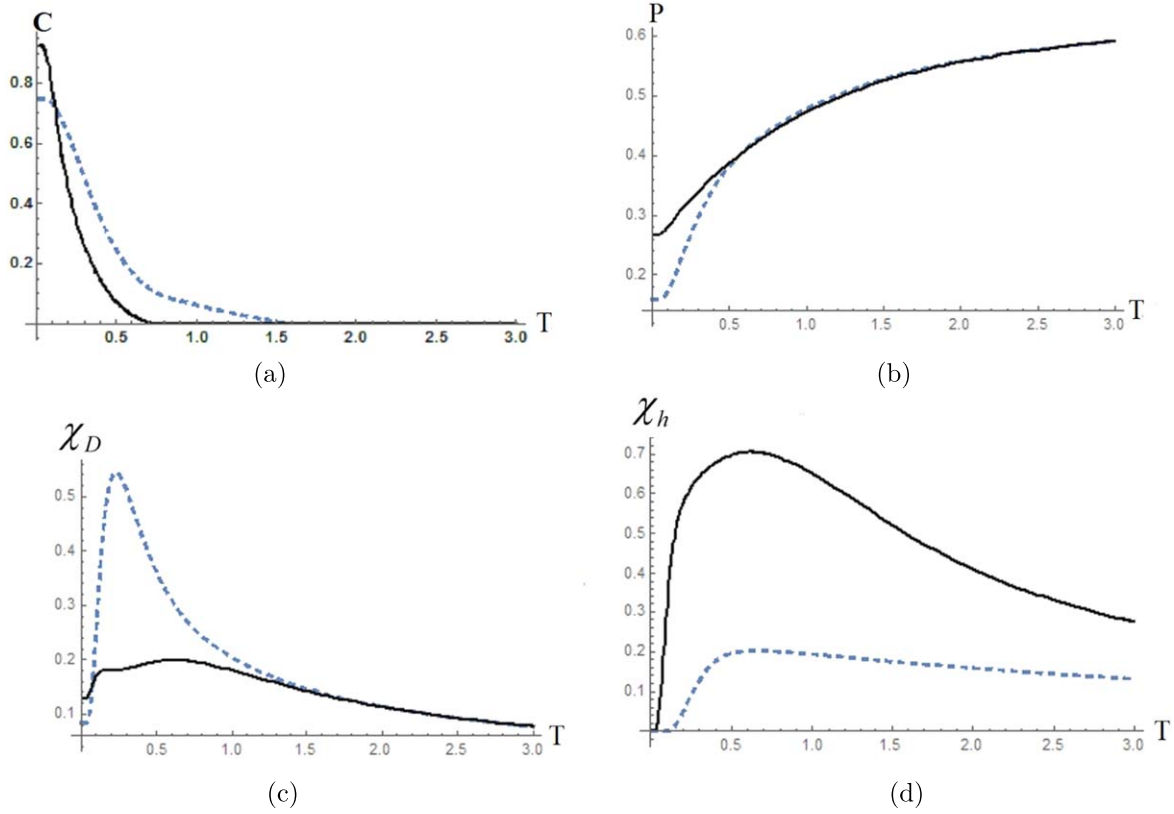


Figure 12. Variations of concurrence (a), particle number (b), particle susceptibility (c) and (d) magnetic susceptibility versus T for $\lambda = h = 0$, $D = 1$ and $N = 3$ with $J = 1$ (dashed) and $J = -1$ (solid).

$|\psi_{ABC}\rangle$ can be factorized as $|\psi_A\rangle|\psi_{BC}\rangle$ or $|\psi_B\rangle|\psi_{AC}\rangle$ or $|\psi_C\rangle|\psi_{AB}\rangle$. In figure 11, the concurrence and the related thermodynamic functions are plotted for three-particle system as a function of D for anti-ferromagnetic and ferromagnetic cases at $T = 0.1$. Unlike the two-particle case, here two critical points are found for $J = 1$. While for $J = -1$, all functions behave in much the same as the two-particle system. At $D = 0$, for $J = 1$, the concurrence is maximum which corresponds to the non-degenerate ground state $|\psi_9\rangle$ with $C(|\psi_9\rangle) = \frac{2}{\sqrt{3}}$. This is due to the fact that $|\psi_9\rangle$, living in the Hilbert space $\mathbb{C}^3 \otimes \mathbb{C}^9$, has the Schmidt form with Schmidt rank three. But in the case of $J = -1$, the ground state is seven-fold degenerated, i.e. it is a mixture of $|\psi_1\rangle, |\psi_2\rangle, |\psi_{10}\rangle, |\psi_{11}\rangle, |\psi_{22}\rangle, |\psi_{24}\rangle$ and $|\psi_{27}\rangle$ states, with zero concurrence.

To explore the low temperature phase of the system, qualitatively, the temperature dependence of the studied functions are plotted in figure 12. At low temperatures, the concurrence of the anti-ferromagnetic case, with $C = \sqrt{\frac{10}{11} - \frac{2}{\sqrt{33}}}$ and $E_{22} = \frac{1}{2}(3 - \sqrt{33})$, is smaller than the ferromagnetic case, with $C = \frac{8}{5\sqrt{3}}$ and $E_{22} = -2$. It is noticeable that, in both cases, non-degenerate ground states occur for $|\psi_{22}\rangle$. By increasing temperature, excited states participate in the density matrix which decreases the strength of the entanglement. For $J = -1$, the magnetic susceptibility is larger than for $J = 1$ case at all temperatures. Except for the magnetic susceptibility, at high temperature, the value of all studied functions for $J = 1$ are larger than for $J = -1$ case and, as depicted in figure 12,

each of the functions converge to a common J independent value at high temperatures. Figure 13(a) shows the results for the generalized concurrence versus D and J for the three-site cluster at a low temperature, $T = 0.01$. The borderlines resemble the borderlines of the particle number function, i.e. figure 13(b), and as is clear from figure 13(c), this resemblance exists for the magnetic susceptibility only for $D < 0$.

Finally, from figure 14 the ability of the generalized concurrence is justified as an order parameter to yield the critical points of this model. The similarity between the magnetization and the generalized concurrence, particularly at the borderline regions, is noticeable.

5. Conclusions

In the present study, we have explored the QPT in the quantum spin-1 Heisenberg system by analyzing the concept of generalized concurrence, magnetization, magnetic susceptibility, particle number and particle susceptibility at finite temperatures. In general, the entanglement decreases as temperature increases. By decreasing temperature, the non-analytic behavior of the concurrence shows two critical points in two-particle anti-ferromagnetic case, with $\lambda = 1$. The Neel state-like behavior has only been observed for the anti-ferromagnetic case at finite temperatures. For the ferromagnetic case, at low temperatures and close to $D = 0$, concurrence and all the studied thermodynamic functions change abruptly.

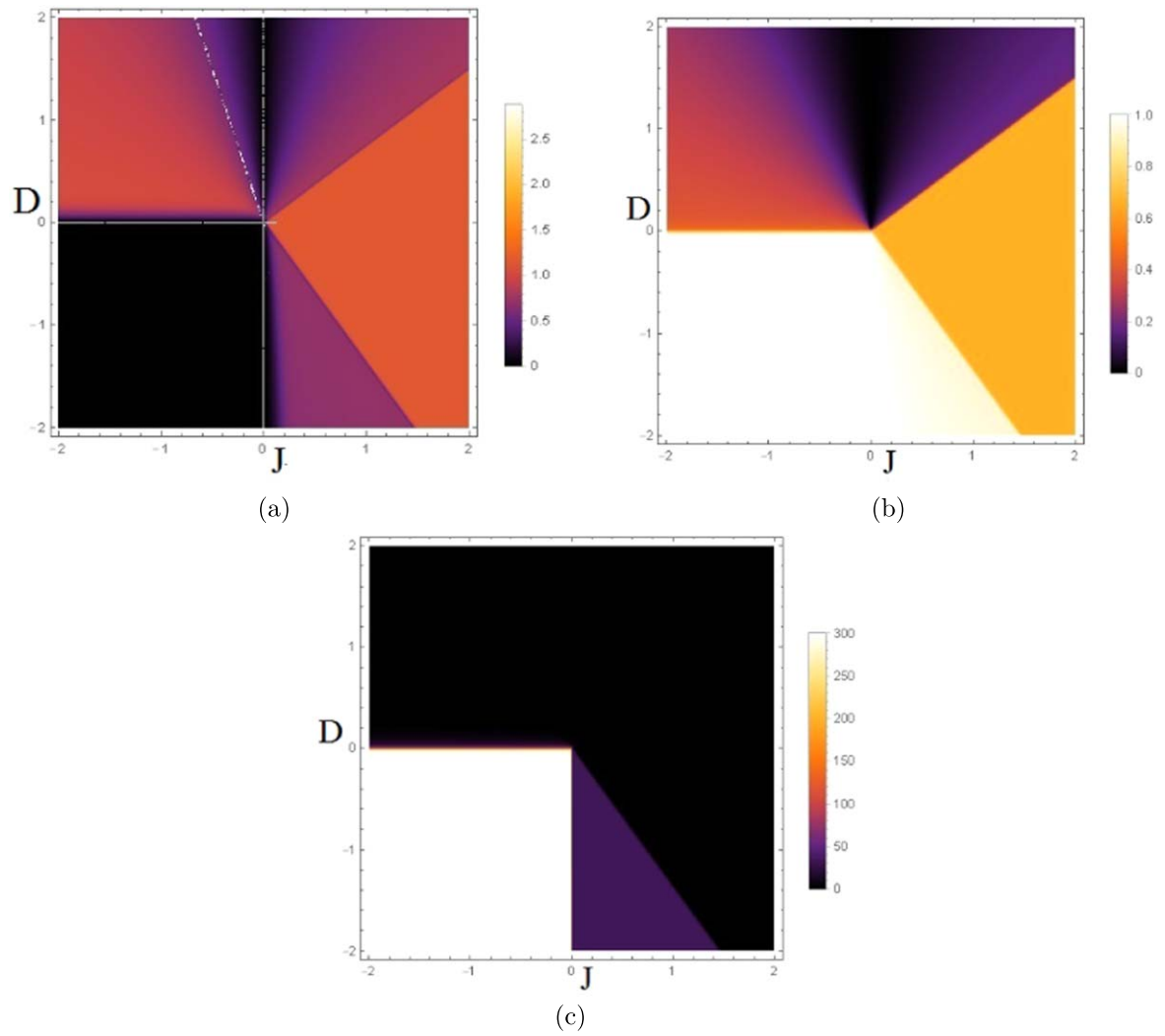


Figure 13. Density of concurrence (a), particle number (b) and magnetic susceptibility (c) versus J and D with $\lambda = 0$ at $T = 0.01$.

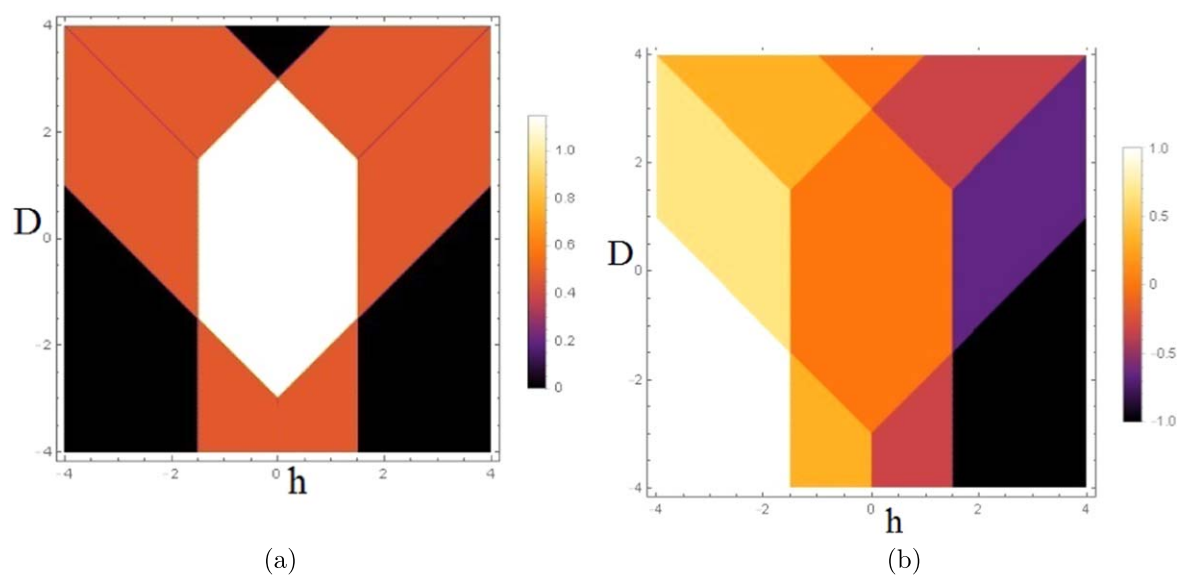


Figure 14. Density of concurrence (a) and magnetization (b) versus h and D for $J = 1$ and $\lambda = 1$ at $T = 0.01$.

Notice that for both $J = \pm 1$ all functions tend to zero at positive large values of D . The critical points for $J = 1$ and $J = -1$ occur at $\lambda_c \simeq 0.3$ and $\lambda_c = -1$, respectively. For the ferromagnetic and the anti-ferromagnetic cases, two ($h_c \simeq \pm 1.83$) and four ($h_c \simeq \pm 1$ and $h_c \simeq \pm 0.45$) critical points have been found, respectively.

For the three-particle system, two critical points are found in the case of $J = 1$ while the $J = -1$ case behaves similar to the two-particle system at zero magnetic field. In zero and non-zero magnetic fields, the critical borderlines of the generalized concurrence and the studied thermodynamic functions coincide, closely. In spite of the fact that we have restricted ourselves to few-particle systems, our results show that this QPTs may be satisfied by the actual thermodynamical systems.

References

- [1] Sachdev S 2013 *Quantum Phase Transitions* (Cambridge: Cambridge University Press)
- [2] Osborne T J and Nielsen M A 2002 *Phys. Rev. A* **66** 032110
- [3] Osterloh A, Amico L, Falcì G and Fazio R 2005 *Nature* **416** 608–10
- [4] Hill S and Wootters W K 1997 *Phys. Rev. Lett.* **78** 5022
- [5] Coffman V, Kundu J and Wootters W K 2000 *Phys. Rev. A* **61** 052306
- [6] Vidal G and Werner R F 2002 *Phys. Rev. A* **65** 032314
- [7] Venuti L C and Zanardi P 2007 *Phys. Rev. Lett.* **99** 095701
- [8] Zhou H Q, Orus R and Vidal G 2008 *Phys. Rev. Lett.* **100** 080601
- [9] Ollivier H and Zurek W H 2001 *Phys. Rev. Lett.* **88** 017901
- [10] Henderson L and Vedral V 2001 *J. Phys. A: Math. Gen.* **34** 6899
- [11] Ferraro A, Aolita L, Cavalcanti D, Cucchietti F M and Acín A 2010 *Phys. Rev. A* **81** 052318
- [12] Dillenschneider R 2008 *Phys. Rev. B* **78** 224413
- [13] Sarandy M S 2009 *Phys. Rev. A* **80** 022108
- [14] Auccaise R, Céleri L C, Soares-Pinto D O, deAzevedo E R, Maziero J, Souza A M, Bonagamba T J, Sarthour R S, Oliveira I S and Serra R M 2011 *Phys. Rev. Lett.* **107** 140403
- [15] Vidal G, Latorre J I, Rico E and Kitaev A 2003 *Phys. Rev. Lett.* **90** 227902
- [16] Tribedi A and Bose I 2009 *Phys. Rev. A* **79** 012331
- [17] Wu L A, Sarandy M S and Lidar D A 2004 *Phys. Rev. Lett.* **93** 250404
- [18] Rojas O, Rojas M, Ananikian N S and de Souza S M 2012 *Phys. Rev. A* **86** 042330
- [19] Wang X 2001 *Phys. Rev. A* **64** 012313
- [20] Kamta G L and Starace A F 2002 *Phys. Rev. Lett.* **88** 107901
- [21] O'Connor K M and Wootters W K 2001 *Phys. Rev. A* **63** 052302
- [22] Sun Y, Chen Y and Chen H 2003 *Phys. Rev. A* **68** 044301
- [23] Yeo Y 2002 *Phys. Rev. A* **66** 062312
- [24] Khveshchenko D V 2003 *Phys. Rev. B* **68** 193307
- [25] Bose S 2003 *Phys. Rev. Lett.* **91** 207901
- [26] Christandl M, Datta N, Ekert A and Landahl A J 2004 *Phys. Rev. Lett.* **92** 187902
- [27] Arnesen M C, Bose S and Vedral V 2001 *Phys. Rev. Lett.* **87** 017901
- [28] Najarbashi G, Balazadeh L and Tavana A 2018 *Int. J. Theor. Phys.* **57** 95
- [29] Balazadeh L, Najarbashi G and Tavana A 2018 *Sci. Rep.* **8** 17789
- [30] Amico L, Fazio R, Osterloh A and Vedral V 2008 *Rev. Mod. Phys.* **80** 517
- [31] Wang X 2002 *Phys. Rev. A* **66** 034302
- [32] Lambert N, Emary C and Brandes T 2004 *Phys. Rev. Lett.* **92** 073602
- [33] Uhlmann A 2000 *Phys. Rev. A* **62** 032307
- [34] Rungta P, Buzek V, Caves C M, Hillery M and Milburn G J 2001 *Phys. Rev. A* **64** 042315
- [35] Audenaert K, Verstraete F and Moor D 2001 *Phys. Rev. A* **64** 052304
- [36] Alberverio S and Fei S M 2001 *J. Opt. B: Quantum Semiclass. Opt.* **3** 1
- [37] Fan H, Matsumoto K and Imai H 2003 *J. Phys. A: Math. Gen.* **36** 4151
- [38] Badziag P, Deuar P, Horodecki M, Horodecki P and Horodecki R 2002 *J. Mod. Opt.* **49** 1289
- [39] Li Y Q and Zhu G Q 2008 *Front. Phys. China* **3** 250–7
- [40] Akhound A, Haddadi S and Motlagh M A C 2019 *Mod. Phys. Lett. B* **33** 1950118
- [41] Chang P-Y, Chu S-k and Ma C-T 2019 *Int. J. Mod. Phys. A* **34** 1950032
- [42] Martín-Martínez E and Menicucci N C 2014 *Class. Quantum Grav.* **31** 214001
- [43] Martín-Martínez E and Menicucci N C 2012 *Class. Quantum Grav.* **29** 224003
- [44] Martín-Martínez E, Smith A R H and Terno D R 2016 *Phys. Rev. D* **93** 044001
- [45] Qiang W-C, Sun G-H, Dong Q and Dong S-H 2018 *Phys. Rev. A* **98** 022320
- [46] Qiang W-C, Sun G-H, Dong Q, C-Nieto O and Dong S-H 2018 *Quantum Inf. Process.* **17** 90
- [47] Xu Y L, Wang L S and Kong X M 2013 *Phys. Rev. A* **87** 012312
- [48] Wootters W K 1998 *Phys. Rev. Lett.* **80** 2245
- [49] Zanardi P and Wang X 2002 *J. Phys. A: Math. Gen.* **35** 7947
- [50] Ferreira A and Lopes dos Santos J M B 2008 *Phys. Rev. A* **77** 034301
- [51] Hao X and Zhu S 2008 *Phys. Rev. A* **78** 044302
- [52] Zheludev A, Tranquada J M, Vogt T and Buttrey D J 1996 *Phys. Rev. B* **54** 7210
- [53] Chen W, Hida K and Sanctuary B C 2003 *Phys. Rev. B* **67** 104401
- [54] Zheludev A, Masuda T, Tsukada I, Uchiyama Y, Uchinokura K, Boni P and Lee S H 2000 *Phys. Rev. B* **62** 8921
- [55] Lou J Z, Xiang T and Su Z B 2000 *Phys. Rev. Lett.* **85** 2380
- [56] Yip S K 2003 *Phys. Rev. Lett.* **90** 250402
- [57] Fan H, Korepin V and Roychowdhury V 2004 *Phys. Rev. Lett.* **93** 227203
- [58] Tzeng Y C, Hung H H, Chen Y C and Yang M F 2008 *Phys. Rev. A* **77** 062321
- [59] Hida K and Chen W 2005 *J. Phys. Soc. Japan* **74** 2090
- [60] Haldane F D M 1983 *Phys. Lett. A* **93** 464
- [61] Griffiths R B 1970 *Phys. Rev. Lett.* **21** 715
- [62] Blume M, Emery V J and Griffiths R B 1971 *Phys. Rev. B* **4** 1071
- [63] Malvezzi A L, Karpat G, Çakmak B, Fanchini F F, Debarba T and Vianna R O 2016 *Phys. Rev. B* **93** 184428
- [64] Wang X, Li H B, Sun Z and Li Y Q 2005 *J. Phys. A: Math. Gen.* **38** 8703–13
- [65] Ren J, Liu G H and You W L 2015 *J. Phys.: Condens. Matter.* **10** 105602
- [66] Lim E W 2019 *Appl. Phys.* arXiv:physics.comp-ph/1904.06542
- [67] Nichols R, Mineh L, Rubio J, Matthews J C F and Knott P A 2019 *Quantum. Sci. Technol.* **4** 045012
- [68] Schollwock U 2005 *Rev. Mod. Phys.* **77** 259
- [69] Schollwock U 2011 *Ann. Phys.* **326** 96

- [70] Pathria P K 1996 *Statistical Mechanics* (Waterloo: Waterloo Univ.)
- [71] Dong S-H, L-Cassou M, Yu J, J-Ángeles F and Rivera A L 2007 *Int. J. Quantum Chem.* **107** 366–71
- [72] Zhang G-F, Liang J-Q, Zhang G-E and Yan Q-W 2005 *Eur. Phys. J. D* **32** 409–12
- [73] Li D-C, Wang X-P and Cao Z-L 2008 *J. Phys.: Condens. Matter.* **20** 325229
- [74] Abgaryan V S, Ananikian N S, Ananikyan L N and Kocharian A N 2011 *Phys. Scr.* **83** 055702
- [75] Zhang G F, Jiang Z T and Abliz A 2011 *Ann. Phys.* **326** 867–75
- [76] Akhtarshenas S J 2005 *J. Phys. A: Math. Gen.* **38** 6777–84